Published in final edited form as:

Bioorg Med Chem Lett. 2012 August 1; 22(15): 5104–5107. doi:10.1016/j.bmcl.2012.05.099.

Synthesis and in vitro evaluation of [^{18}F](*R*)-FEPAQ: A potential PET ligand for VEGFR2

Jaya Prabhakaran[a,*], **Victoria Arango**[a,b], **Vattoly J. Majo**[a], **Norman R. Simpson**[a,b], **Suham A. Kassir**[b], **Mark D. Underwood**[a,b], **Hanish Polavarapu**[a], **Jeffrey N. Bruce**[c], **Peter Canoll**[c], **J. John Mann**[a,b,d], and **J. S. Dileep Kumar**[a,b]

[a]Division of Molecular Imaging and Neuropathology, Department of Psychiatry, Columbia University College of Physicians and Surgeons, New York, USA

[b]New York State Psychiatric Institute, New York, USA

[c]Department of Neurology, Columbia University, New York, USA

[d]Department of Radiology, Columbia University College of Physicians and Surgeons, New York, NY 10032, USA

Abstract

Synthesis and in vitro evaluation of [^{18}F](*R*)-*N*-(4-bromo-2-fluorophenyl)-7-((1-(2-fluoroethyl)piperidin-3-yl)methoxy)-6-methoxyquinazolin-4-amine ((*R*)-[^{18}F]FEPAQ or [^{18}F]**1**), a potential imaging agent for the VEGFR2, using phosphor image autoradiography are described. Synthesis of **2**, the desfluoroethyl precursor for (*R*)-FEPAQ was achieved from *t*-butyl 3-(hydroxymethyl)piperidine-1-carboxylate (**3**) in five steps and in 50% yield. [^{18}F]**1** was synthesized by reaction of sodium salt of compound **2** with [^{18}F]fluoroethyl tosylate in DMSO. The yield of [^{18}F]**1** was 20% (EOS based on [^{18}F]F^-) with >99% radiochemical purity and specific activity of 1–2 Ci/μmol (n = 10). The total synthesis time was 75 min. The radiotracer selectively labeled VEGFR2 in slide-mounted sections of human brain and higher binding was found in surgically removed human glioblastoma sections as demonstrated by in vitro phosphor imager studies. These findings suggest [^{18}F]**1** may be a promising radiotracer for imaging VEGFR2 in brain using PET.

Keywords

VEGFR2; Radiotracer; PET; Glioma; Bioimaging

A key protein in the regulation of angiogenesis and vasculogenesis is vascular endothelial growth factor (VEGF), which is overexpressed in virtually all human tumors.[1–6] In addition to tumors, VEGF exerts neuroprotective actions directly through the inhibition of programmed cell death (PCD) or apoptosis, and the stimulation of neurogenesis.[7–9] Apart from angiogenesis, VEGF is a mediator of multiple processes enhancing blood brain barrier (BBB) permeability for glucose, and antioxidant activation, which indirectly results in

*Corresponding author: Fax: +1 212 543 1054. jp2155@columbia.edu (J. Prabhakaran).

neuroprotection.[10] VEGF protects against neuronal death from hypoxia and glucose deprivation.[7,8,11,12] VEGF signaling through VEGFR2 was also shown to be required for antidepressants (fluoxetine, desipramine) to increase cell proliferation. Chronic antidepressant administration increases VEGF expression in both neurons and endothelial cells in the hippocampus. [13–45] Thus, VEGF is a key component in the regulation of neuron and vessel growth in brain and other pathologies. There are excellent reviews that detail the therapeutic potential of VEGF and its receptors in CNS.[6,7,16,17] VEGF effects are mediated by a family of receptor tyrosine kinases (TKs), including VEGFR-1 (Flt-1), VEGFR-2 (KDR or Flk-1) and VEGFR-3 (Flt-4).[7,18] Of these, VEG-FR-2 appears to mediate almost all of the known cellular responses to VEGF. Antagonism of the VEGF pathway results in inhibition of angiogenesis and tumor growth in a number of tumor model systems. [19–21] Although there has been significant advance in the imaging of tumors, there is a lack of agents for imaging and quantifying indices of angiogenesis. Inhibiting VEGF expression and interfering with angiogenesis may be a useful treatment target for tumors. It is reported that tumor perfusion changes dynamically during anti-VEGF treatment and that specific molecular markers in tumors and vasculature can be correlated with these perfusion changes.[22–25] Noninvasive imaging of VEGFR2 is of great potential clinical importance, as it may identify factors contributing to tumor resistance. Positron Emission Tomography (PET) imaging of VEGFR2 in tumor patients at baseline and in response to chemotherapy treatment may also provide novel information about the mechanisms that contribute to therapy resistance, and allow more effective use of VEGF inhibition. The multimodality molecular imaging of VEGF and VEGFR with radiotracers have recently been reviewed.[26–28] Efforts to image VEGF/VEGFR first focused VEGFR-specific uptake and the dynamic nature of the receptor expression in tumors as well as biological responses on tracing the distribution of the ligand by targeting with anti-VEGF antibodies labeled with 124-I and 89-Zr.[29–31] VEGFR-specific uptake and the dynamic nature of the receptor expression in tumors as well as biological responses to myocardial infarction and ischemia have been successfully demonstrated using these tracers.[31–33] However, imaging the expression of a ligand in circulation using long-lived antibodies as imaging probes requires waiting days until the unbound tracer has cleared sufficiently from the blood and the nonspecific uptake has declined sufficiently for good target/nontarget contrast. Mutated-VEGF121 (VEGFDEE) has also been developed to increase specificity for VEGFR2 and the results obtained were promising for potential translation to clinical studies. [34] However, these peptide ligands do not cross BBB and hence the tracers are limited to imaging studies outside the brain. An understanding of the potential therapeutic value associated with binding to VEGFR2 in brain requires development of selective non-peptide PET ligands. Therapeutic drugs that act by binding to VEGFR2 can be evaluated and their therapeutic dose determined by an occupancy study using such a specific PET tracer. A specific PET tracer could also serve as a biological marker for angiogenesis and for the evaluation of diseases in which changes in VEGF receptor binding occurs. For example, VEGFR2 changes in tissue proliferation or angiogenesis can be quantified in vivo using PET. However, there is currently no good radiotracer for the measurement of VEG-FR2 binding expression in tumors and to monitor their role in angiogenesis. Racemic [^{11}C]PAQ was reported as the first VEGFR2 selective PET tracer which was proved specific for kidney tumors in rodents.[35] Radiolabeling of racemic [^{18}F]sunitinib, [^{11}]vandetanib and

[^{11}C]chloro-vandetanib has been recently reported, however, biological evaluation of these tracers are not reported yet.[36] All these radiotracers are 4- or 3-piperidinyl analogues of vandetanib (rINN, Caprelsa ZD6474), the first VEGFR2 drug approved by FDA.[37,38] Moreover, it has been reported that the (*R*)-enantiomer of vandetanib is 10-fold more active than (*S*)-enantiomer, also there is a better selectivity of (*R*)-enantiomer with respect to EGFR and VEGFR1.[39] Herein we report the synthesis and evaluation of (*R*)-enantiomer of a viable [F-18]analogue of PAQ [^{18}F]fluoroethyl PAQ ([^{18}F]FEPAQ, [^{18}F]**1**) as a potential candidate for VEGFR2 imaging with PET.

We synthesized (*R*)-fluoroethyl-PAQ ((*R*)-FEPAQ) and the corresponding desfluoroethyl-PAQ with appropriate modifications of literature methods (Scheme 1).[35,39] In brief, reaction of 4-hydroxy-6-methoxyquinazolin-7-yl benzoate (**5**) with $POCl_3$ and *N*,*N*-diisopropylethyl amine and the coupling of the intermediate choroquinoline formed with 4-bromo-2-fluoroaniline (**6**) in one pot, afforded 4-((4-bromo-2-fluorophenyl)amino)-6-methoxy quinazolin-7-ol (**7**) in 70% yield.[39] Compound **7** upon reaction with (*R*)-*tert*-butyl 3-((tosyloxy)methyl)piperidine-1-carboxylate (**4**), which in turn was obtained by the tosylation of commercial (*R*)-*tert*-butyl 3-(hydroxymethyl)piperidine-1-carboxylate (**3**), resulted in the isolation of BOC protected precursor using column chromatography (2–3% methanol in methylene chloride). The BOC protection was removed by treatment with trifluoro acetic acid in methylene chloride (1:1) to afford the radiolabeling precursor (*R*)-desfluoroethyl-PAQ (**2**) in 50% yield.[35] The nonradioactive standard (*R*)-FEPAQ (**1**) was obtained by reaction of compound **2** with fluoroethyl-bromide in 60% yield.[48] The VEGFR2 binding affinity (IC_{50}) of compound **1** was found to be 40 nM based on VEG-FR2 incubation mobility-shift KDR kinase assay using microfluidic chip to measure the conversion of a fluorescent peptide substrate to a phosphorylated product.[49] The radiolabeling of compound **1** was achieved in two steps (Scheme 1).[40] The radiolabeling was attempted under several conditions and the optimal method we adopted is present here. [^{18}F]Fluoroethyl tosylate ([^{18}F]FE-OTs) is prepared first by reacting [^{18}F]F^- with ethylene glycol ditosylate using a modified procedure reported elsewhere.[41] The crude product was purified using solid phase extraction using C-18 Sep-Pak® to yield 70% of [^{18}F]FE-OTs. The [^{18}F]FE-OTs obtained is azeotropically dried and reacted with freshly prepared sodium salt of **2** in DMSO. The radiolabeled product was further purified using semi-preparative HPLC to afford [^{18}F]**1** in 20 ± 5% yield (n = 10). The chemical identity of [^{18}F]**1** was confirmed by co-injecting with nonradiolabeled (*R*)-**1** by HPLC technique. The total time required for the radiosynthesis was 75 min. The radiochemical purity of [^{18}F]**1** was found to be >99% and the specific activity in the ranges of 1–2 Ci/μmol (EOB).

After synthesizing the radioligand in consistent yield and sufficient specific activity, [^{18}F]**1** was tested in surgically removed human glioblastoma using phosphor image autoradiography to determine its binding to VEGFR2 (Fig. 1).[42] We choose glioblastoma model for the evaluation of [^{18}F]**1** because it is the most common brain malignancy, with high levels of VEGF and VEGFR2 expression when compared to other non-neural solid cancers.[43–45] Additionally, studies in animal models have shown that VEGFR2 inhibitors suppress the growth of gliomas in vivo and cause regression of blood vessels.[46,47] Frozen brain sections were used for the phosphor image study in quadruplicate. Slide-mounted

sections were incubated in Tris buffer (pH 7.4) containing 0.18 nM of [^{18}F]**1** for 60 min at room temperature. Adjacent sections were incubated with ZM-323881 or (*R*)-PAQ, the two known selective VEGFR2 antagonists (1 μM) to determine nonspecific binding. After the incubation, sections were washed with ice-cold buffer and slides were quickly dried under a stream of cold air and exposed to a phosphor-imaging screen with high- and low-activity standards for 60 min. Screens are scanned with a Packard Cyclone phosphor-imaging system and analyzed with OptiQuant Acquisition and Analysis software (Packard). Displacement of total binding was observed with both VEGFR2 ligands as evident from Figure 1.

In summary, we successfully synthesized [^{18}F]**1**, a potential imaging agent for VEGFR2. The total time required for the radiosynthesis was 75 min from EOS using [^{18}F]FE-OTs in DMSO. [^{18}F]**1** was obtained in 20 ± 5% yield (EOS) with excellent radiochemical purities and specific activity. Phosphor image studies indicate that this newly developed [^{18}F]**1** ligand binds to VEGFR2 in surgically removed human glioma. The results obtained indicate the feasibility of using [^{18}F]**1** as a potential imaging agent to visualize VEGFR2 in brain using PET.

Acknowledgments

This work was partially supported by Clinical and Translational Science (CTSA) award, Columbia University Medical Center (to J.P.).

References and notes

1. Waldner MJ, Neurath MF. Expert Opin Ther Targets. 2012; 16:5. [PubMed: 22239434]
2. Vitale G, Dicitore A, Gentilini D, Cavagnini F. Cancer Biol Ther. 2010; 9:694. [PubMed: 20339315]
3. Dowlati AJ. Clin Oncol. 2010; 28:185.
4. Ellis LM, Hicklin DJ. Nat Rev Cancer. 2008; 8:579. [PubMed: 18596824]
5. Smith NR, Baker D, James NH, Ratcliffe K, Jenkins M, Ashton SE, Sproat G, Swann R, Gray N, Ryan A, Jürgensmeier JM, Womack C. Clin Cancer Res. 2009; 15:4138. [PubMed: 19509160]
6. Ferrara N, Darren DW, Roy HS, James AL. Antiangiogenic Cancer Ther. 2008:23.
7. Rosenstein, JM.; Kruin, JM.; Ruhrberg, C. VEGF in the Nervous System. In: Ruhrberg, C., editor. VEGF in Development. Landes Bioscience and Springer Science; 2008. p. 91-103.
8. Almodovar CR, Lambrechts D, Mazzone M, Carmeliet P. Physiol Rev. 2009; 89:607. [PubMed: 19342615]
9. Góra KK, Jośko JT. Folia Neuropathol. 2005; 43:31. [PubMed: 15827888]
10. Abbott JN, Rönnbäck L, Hansson E. Nat Rev Neurosci. 2006; 7:41. [PubMed: 16371949]
11. Jin KL, Mao XO, Greenberg DA. PNAS. 2000; 97:10242. [PubMed: 10963684]
12. Yun H, Lee M, Kim SS, Ha J. J Biol Chem. 2005; 280:9963. [PubMed: 15640157]
13. Fournier NM, Duman RS. Behav Brain Res. 2012; 227:440. [PubMed: 21536078]
14. Kodama M, Fujioka T, Duman R. Biol Psychiatry. 2008; 56:570. [PubMed: 15476686]
15. Couillard -DS, Wuertinger C, Kandasamy M, Caioni M, Stadler K, Aigner R, Bogdahn U, Aigner L. Mol Psychiatry. 2009; 14:856. [PubMed: 19139747]
16. Ian Z. Neurosignals. 2005; 14:207. [PubMed: 16301836]
17. Cao L, Jiao X, Zuzga DS, Liu Y, Fong DM, Young D, During MJ. Nat Genet. 2004; 36:827. [PubMed: 15258583]
18. Roskoski S Jr. Biochem Biophys Res Commun. 2008; 375:287. [PubMed: 18680722]
19. Wahl O, Oswald M, Tretzel L, Herres E, Arend J, Efferth T. Curr Med Chem. 2011; 18:3136. [PubMed: 21671856]

20. Furuya M, Nagahama K, Ishizu A, Otsuka N, Nagashima Y, Aoki I. Front Biosci. 2011; E3:549.
21. Ho TQ, Kuo CJ. Int J Biochem Cell Biol. 2007; 39:1349. [PubMed: 17537667]
22. Rehman S. Oncologist. 2005; 10:92. [PubMed: 15709211]
23. Keunen O, Johansson M, Oudin A, Sanzey M, Abdul Rahim SA, Fack F, Thorsen F, Taxt T, Bartos M, Jirik R, Miletic H, Wang J, Stieber D, Stuhr L, Moen I, Rygh CB, Bjerkvig R, Niclou SP. PNAS. 2011; 108:3749. [PubMed: 21321221]
24. Weis SM, Cheresh DA. Nat Med. 2011; 17:1359. [PubMed: 22064426]
25. Schroeder CP, Hospers GAP, Willemse PHB, Perik PJ, de Vries EFJ, Jager PL, van der Graaf WTA, Lub-de Hooge MN, de Vries EGE. Cancer Metastasis Biol Treat. 2007; 11:307.
26. Cai W, Chen X. J Nucl Med. 2008; 49:113S. [PubMed: 18523069]
27. Hicks JW, VanBrocklin HF, Wilson AA, Houle S, Vasdev NS. Molecules. 2010; 15:8260. [PubMed: 21079565]
28. Collingridge DR, Carroll VA, Glaser M, Aboagye EO, Osman S, Hutchinson OC, Barthel H, Luthra SK, Brady F, Bicknell R, Price P, Harris AL. Cancer Res. 2002; 62:5912. [PubMed: 12384557]
29. Nagengast WB, de Vries EG, Hospers GA, Mulder NH, de Jong JR, Hollema H, Brouwers AH, van Dongen GA, Perk LR, Lub-de Hooge MN. J Nucl Med. 2007; 48:1313. [PubMed: 17631557]
30. Backer MV, Levashova Z, Patel V, Jehning BT, Claffey K, Blankenberg FG, Backer JM. Nat Med. 2007; 13:504. [PubMed: 17351626]
31. Rodriguez-Porcel M, Cai W, Gheysens O, Willmann JK, Chen K, Wang H, Chen IY, He L, Wu JC, Li ZB, Mohamedali KA, Kim S, Rosenblum MG, Chen X, Gambhir SS. J Nucl Med. 2008; 49:667. [PubMed: 18375924]
32. Willmann JK, Chen K, Wang H, Paulmurugan R, Rollins M, Cai W, Wang DS, Chen IY, Gheysens O, Rodriguez PM, Chen X, Gambhir SS. Circulation. 2008; 117:915. [PubMed: 18250264]
33. Wang H, Cai W, Chen K, Li ZB, Kashefi A, He L, Chen X. Eur J Nucl Med Mol Imaging. 2007; 34:2001. [PubMed: 17694307]
34. Wang JQ, Miller KD, Sledge GW, Zheng QH. Bioorg Med Chem Lett. 2005; 15:4380. [PubMed: 16019210]
35. Gao M, Lola CM, Wang M, Miller KD, Sledge GW, Zheng QH. Bioorg Med Chem Lett. 2011; 21:3222. [PubMed: 21549594]
36. Samén E, Thorell JO, Lu L, Tegnebratt T, Holmgren L, Stone-Elander S. Eur J Nucl Med Mol Imaging. 2009; 36:1283. [PubMed: 19288096]
37. Commander H, Whiteside G, Perry C. Drugs. 2011; 71:1355. [PubMed: 21770481]
38. Langmuir PB, Yver A. Clin Pharmacol Ther. 2012; 91:71. [PubMed: 22158569]
39. Hennequin LF, Stokes ES, Thomas AP, Johnstone C, Plé PA, Ogilvie DJ, Wedge SR, Kendrew J, Curwen JO. J Med Chem. 2002; 45:1300. [PubMed: 11881999]
40.
Radiosynthesis of [^{18}F]**1**: To an aqueous [^{18}F]fluoride solution were added a solution containing kryptofix®2.2.2. (11 mg, 0.03 mmol), potassium carbonate (2 mg, 0.014 mmol) in 0.2 mL of 95:5 acetonitrile/water. The mixture was dried in a stream of argon at 95 °C for 10 min, followed by azeotrope with acetonitrile (3 × 0.5 mL) for three times. To the dried kryptofix®2.2.2./[^{18}F] fluoride complex, 4 mg ethyleneglycol-1,2-ditosylate in 1 mL acetonitrile was added and heated in a sealed vial for 10 min. At the end of the reaction, the crude product was diluted with 10 mL DI water and passed through an activated C-18 Sep-Pak®. The C-18 Sep-Pak® cartridge was further washed with 4 mL hexane and dried under argon. The Sep-Pak® was then eluted with 2 mL ether to obtain [^{18}F]FEOTs in 70%. The ether solution was dried under argon, added with 4 mg of freshly prepared sodium salt of (R)-**2** in 0.25 mL DMSO and heated for 20 min at 90 °C (The sodium salt was prepared by dissolving 4 mg of compound **2**, dissolved in 0.5 mL of acetonitrile followed by addition of 2–4 μL of 5 M NaOH solution. The mixture was vortexed and the solvent was removed azeotropically at 90 °C under a stream of argon. The sodium salt thus obtained was

dissolved in 0.25 mL of DMSO for further reaction). The crude product was diluted with 0.25 mL of acetonitrile and was directly injected into a semi preparative RP-HPLC (Phenomenex C18, 10 × 250 mm, 10) and eluted with acetonitrile: 0.1 M ammonium formate solution (35:65) at a flow rate of 10 mL/min. The precursor eluted after 6–7 min during the HPLC analysis. The product fraction with a retention time of 10–11 min based on γ-detector was collected, diluted with 50 mL of deionized water, and passed through a C-18 Sep-Pak® cartridge. Reconstitution of the product in 1 mL of absolute ethanol afforded [^{18}F]**1** (20 ± 5% yield, based on [^{18}F]F^- at EOS). A portion of the ethanol solution was analyzed by analytical RP-HPLC (Phenomenex, Prodigy ODS(3) 4.6 × 250 mm, 5 m; mobile phase: acetonitrile/0.1 M ammonium formate; 40:60, flow rate: 2 mL/min, retention time: 7 min, wavelength: 254 nm) to determine the specific activity and radiochemical purity. The ethanol solution of [^{18}F]**1** was used for further studies.

41. Bauman A, Piel M, Schirrmacher R, Rosch F. Tetrahedron Lett. 2003; 44:9165.Block D, Coenen HH, Stocklin G. J Labelled Compd Radiopharm. 1987; 25:201.

42.

In vitro phosphor image with [^{18}F]**1**: The in vitro experiments will be performed using pathologically identified surgically removed glioma tissues. The frozen glioma tissues were sectioned (20 μm) were collected onto glass slides and were used for the phosphor image studies. Four sections each for total and nonspecific binding were assayed. The slides mounted sections were brought to room temperature and were incubated with 50 mM Tris–HCl, 5 mM of KCl and 150 mM of NaCl at pH 7.4 containing [^{18}F]**1** (0.1 nM) for 1 h. The adjacent sections were incubated with 1 mM of ZM 323881 ·HCl or 1 mM of (*R*)-PAQ for 1 h to determine non specific binding. After the incubation, sections were washed with ice-cold buffer containing 50 mM Tris-buffer (pH 7.4) at 4 °C and briefly dipped in ice-cold water to remove salts. Slides were quickly dried under a stream of cold air and exposed to a phosphor-imaging screen (Packard, ST screen wrapped in Mylar film) with high- and low-activity standards (American Radiolabeled Chemicals) for 60 min. Screens are scanned with a Packard Cyclone phosphor-imaging system and analyzed with OptiQuant Acquisition and, Analysis software (Packard).

43. Sathornsumetee S, Rich JN. Curr Pharm Res. 2007; 13:3545.

44. Oka N, Soeda A, Inagaki A, Onodera M, Maruyama H, Hara A, Kunisada T, Mori H, Iwama T. Biochem Biophys Res Commun. 2007; 360:553. [PubMed: 17618600]

45. Peles E, Lidar Z, Simon AJ, Grossman R, Nass D, Ram Z. Neurosurgery. 2004; 55:562. [PubMed: 15335423]

46. Sandstrom M, Johansson M, Bergstrom P, Bergenheim AT, Henriksson R. J Neurooncol. 2008; 88:1. [PubMed: 18228115]

47. Lamszus K, Brockmann MA, Eckerich C, Bohlen P, May C, Mangold U, Fillbrandt R, Westphal M. Clin Cancer Res. 2005; 11:4934. [PubMed: 16000592]

48.

^{1}H NMR ($CDCl_3$, 300 MHz): 8.7 (s, 1H), 8.5 (m, 1H), 7.4 (br s, 2H), 7.3 (m, 1H), 7.0 (s, 1H), 4.7 (m, 1H), 4.6 (m, 1H), 4.1 (m, 2H), 3.9 (s, 3H), 3.2 (m, 1H), 3.0–2.6 (m, 6H), 2.4–1.8 (m, 4H); HRMS (*m/z* calcd $C_{23}H_{25}BrF_2N_4O_2$; 507.1214; found 507.1203); HPLC (Phenomenex, Prodigy ODS(3) 4.6 × 250 mm, 5μ; mobile phase: acetonitrile/0.1 M ammonium formate; 40:60, flow rate: 2 mL/min, retention time: 7 min, wavelength: 254 and 270 nm, >99% purity.

49.

KDR in vitro enzymatic binding assay was performed by Calipers Life Sciences Discovery and Alliance services (http://www.caliperls.com/products/contract-research/in-vitro/kinases/kdr-vegfr2-flk1-h.htm).

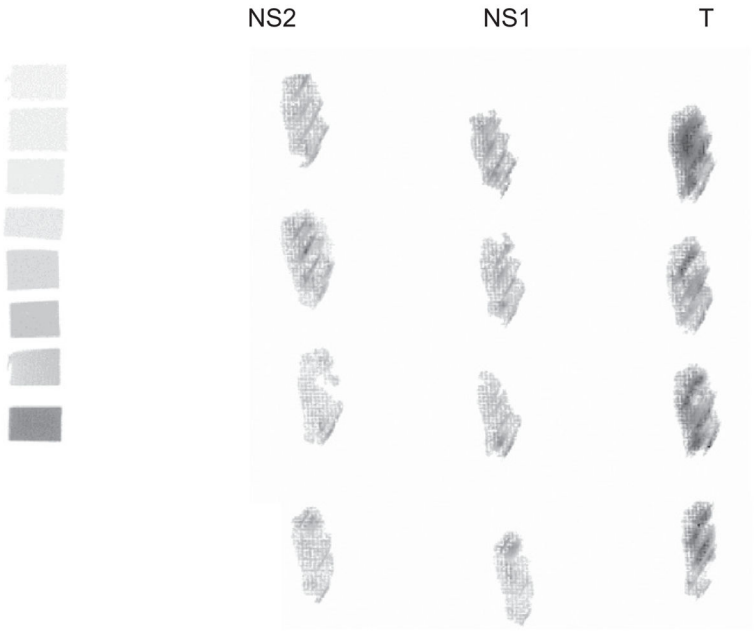

Figure 1.

Phosphor image of [^{18}F]**1** in glioma sections. T: total binding; NS1: nonspecific binding defined by blockade with ZM-323881; NS2: nonspecific defined by blockade with (*R*)-PAQ.

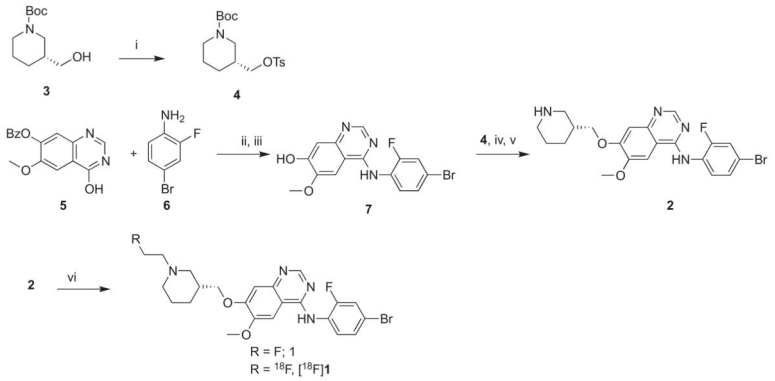

Scheme 1.

Synthesis and radiosynthesis of (*R*)-FEPAQ and (*R*)-[^{18}F]FEPAQ. Reagents and conditions: (i) $(Ts)_2O$, THF, 6 h; (ii) $POCl_3$, CH_2Cl_2; (iii) K_2CO_3, THF; (iv) **4**, K_2CO_3, THF; (v) TFA, CH_2Cl_2; (vi) fluoroethyl bromide/[^{18}F]FEOTs, DMSO.